Appendix B – A Series of Other Studies

Bridgman Solidification

Directional Solidification:
Heating a 2-phase alloy to its liquidus and then cooling slowly from one side to directionally solidify the second phase.

Microgravity is needed to avoid sedimentation of the dendrites during processing (different densities).

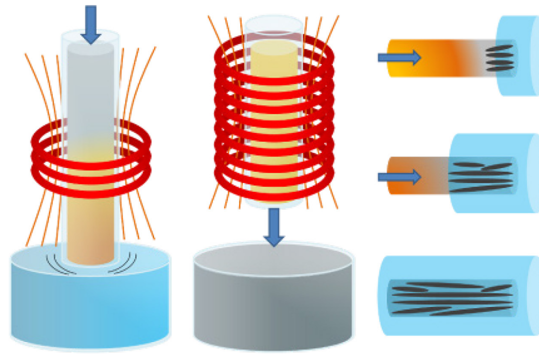

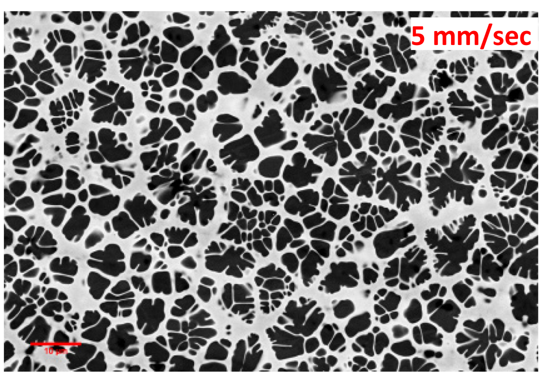

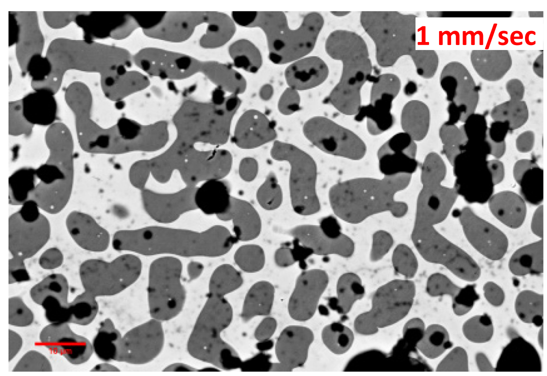

A 1.5 inch diameter graphite rod had a hole bored in the center. A quartz tube containing a thin DV1 rod was then inserted into the center, and the susceptor was heated via RF induction heating. The susceptor was used since the DV1 rods were too thin to couple efficiently with the low frequency of the power supply. A container of a molten fusible alloy was used as a quenching bath. The quartz tubes containing DV1 rods were lowered at differing rates (5 mm/sec and 1 mm/sec) into the metal bath. This was intended to initiate directional solidification, with the dendrites growing from the molten alloy bath towards the graphite susceptor. Unfortunately, no texturing was observed, although the alloy being annealing for longer did have substantial coarsening of the dendrites. It is likely the liquidus temperature was not reached to fully remelt the dendrites. Instead, the existing dendrites coarsened. Dark spots are due to polishing debris adhered onto the surface. Images were taken in QBSD mode at 2500x. Experiments were performed with Henry Kozachkov and Doug Hofmann.

Quasistatic Compression Testing of a Single Eggbox's Pyramid

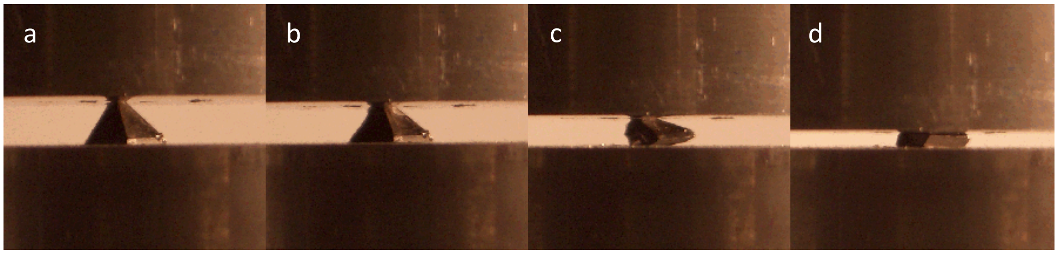

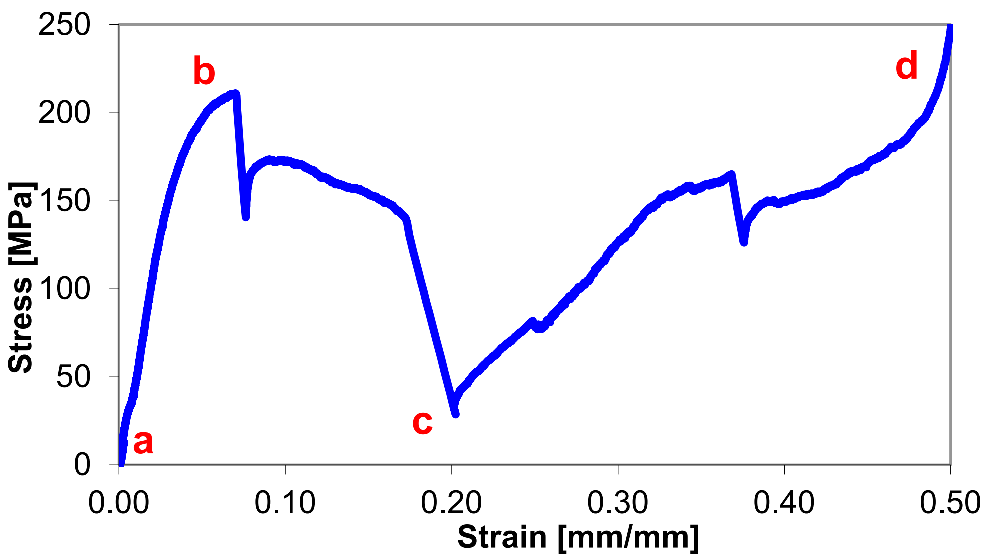

A single eggbox from structures used in Chapters 2-4. The stress supported by a single pyramid should be the maximum stress achievable by an eggbox structure. The difference between the stress supported by a sheet and a single eggbox indicates how much strength is lost due to geometry. It is known from previous chapters the 1 mm offset between pyramids allows for torqueing to occur which lowers the strength of welded structures. This was also seen in the images published in Joe Schramm's thesis.

The slight change in slope of the stress-strain curve is due to the pyramid's tip sinking into the hardened steel platens as the Instron was loaded. The pyramid is harder than the platens, so it is not surprising it is able to dent them significantly. As point (b) is approached the pyramid begins to yield and plastic deformation behavior is apparent. This signifies the spacing of dendrites in the composite pyramid is on the appropriate length scale to arrest shear band growth.

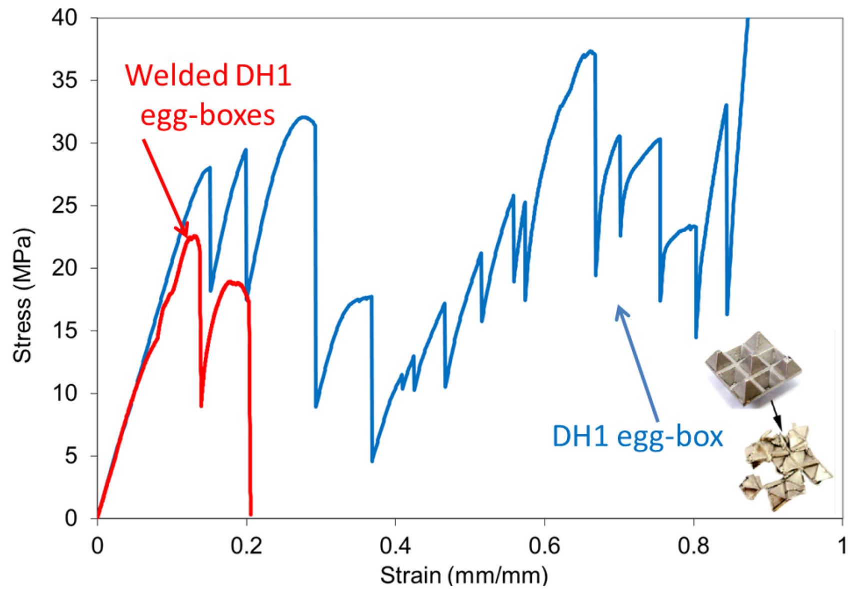

Above, Figure 3-3 is recreated to highlight the difference between performance in a single pyramid and a full eggbox structure. Each structure exhibits significant recovery after the first failure event. The single pyramid supports significantly more stress, although this is likely an effect of the eggbox geometry having both ‘up’ and ‘down’ pyramids. In a 3x3 eggbox, the entire load would be supported by 4 pyramids (in the inset figure, each would be facing down). For this reason, the measured stress is lower than that actually experienced by the actual 4 mm^2 of tip which is in contact with the platens. The pyramid was still, however, able to withstand more than seven times as much stress as a whole eggbox structure, a difference which is not made up for in geometry. For this reason, we can conclude the eggbox design used has further room for optimization.

Metallic Glass Wires

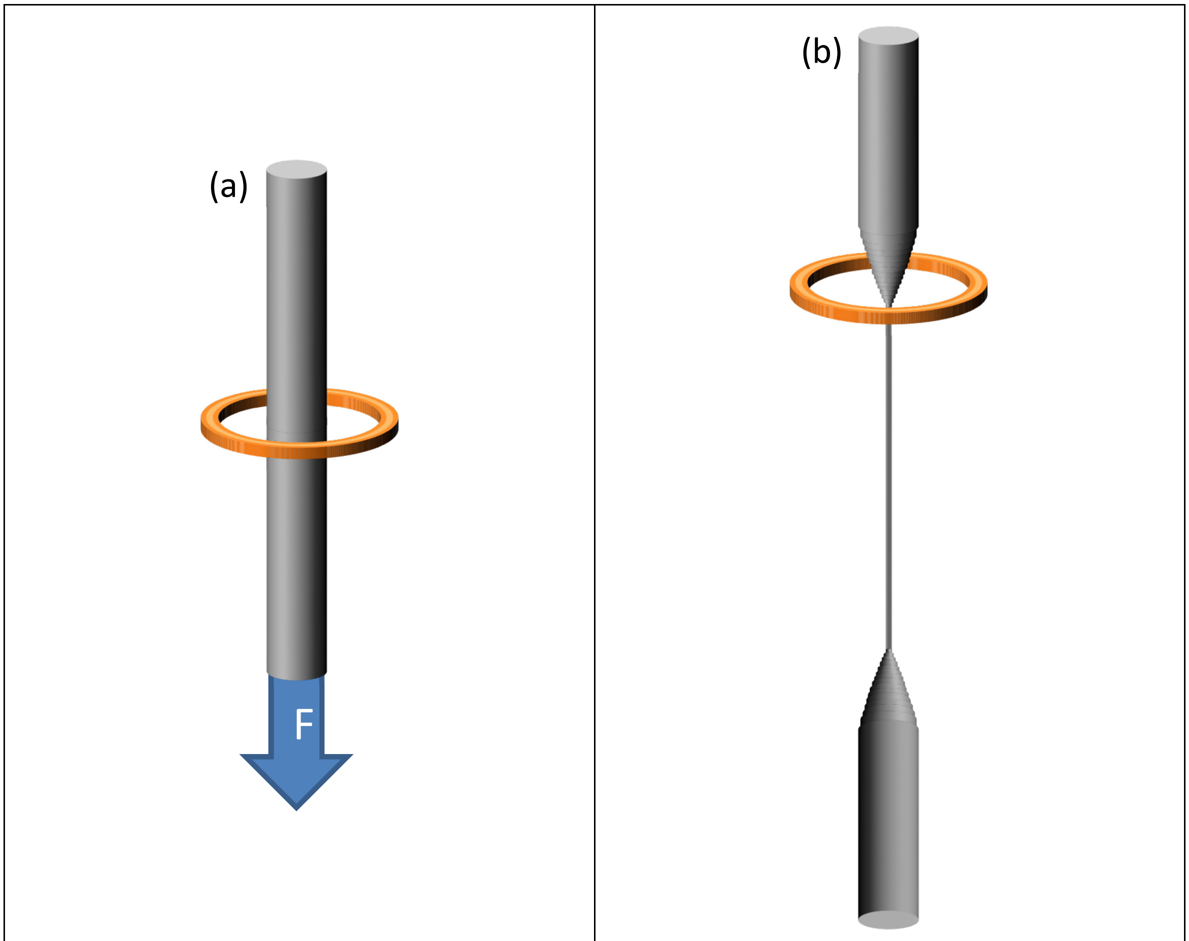

(a) Initially a metallic glass cylinder is preloaded with a force (e.g. a mass being pulled by gravity). A RF induction coil is placed around the cylinder.
(b) Localized heating by the RF coil causes the cylinder to heat above the glass transition temperature and, with sufficient force, flow occurs. As the coil thins it becomes more efficient at radiating heat since the surface area to volume ratio dramatically increases. Eventually the wire becomes thin enough the RF coil can no longer efficiently couple to the glass, and no more energy can be put into the system. At this point the wire stops drawing further.

The actual drop tower height was in excess of 18 inches.

A series of drop tower experiments. Wires were made with gauge sections of over 0.5 m. Different lengths and thicknesses were achieved by modifying the applied force and heating power.

This series of experiments were performed with Allison Kunz and Doug Hofmann.

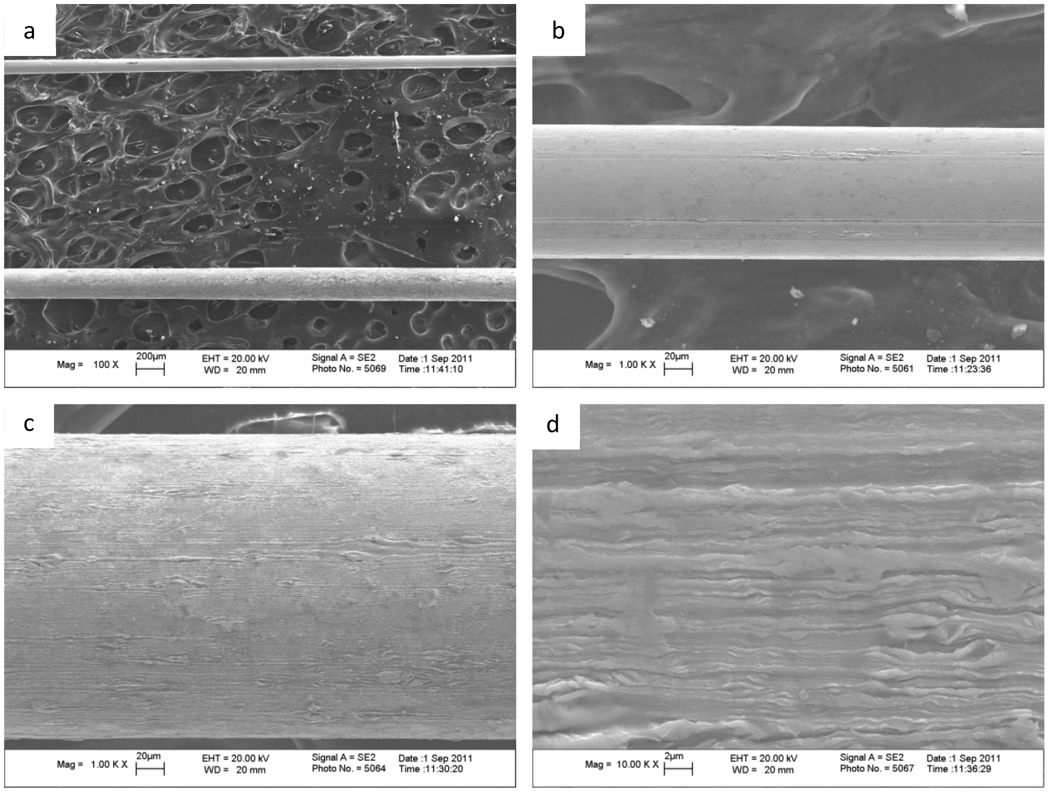

GHDT ($Zr_{35}Ti_{30}Be_{27.5}Cu_{7.5}$) wires.

(a) An overview of two wires. The top one is approximately 100 μm and the bottom is approximately 225 μm.

(b) 1000x of the top wire

(c) 1000x of the bottom wire

(d) 10000x of the bottom wire

Neither wire was brittle, which indicates they had likely fully vitrified. Thinner wires tended to have a much smoother surface. The thinner wire likely reached both a higher temperature and had its surface smoothed out due to imperfections smearing out over a longer length. Rods were initially fabricated via suction casting which leaves a moderately rough surface

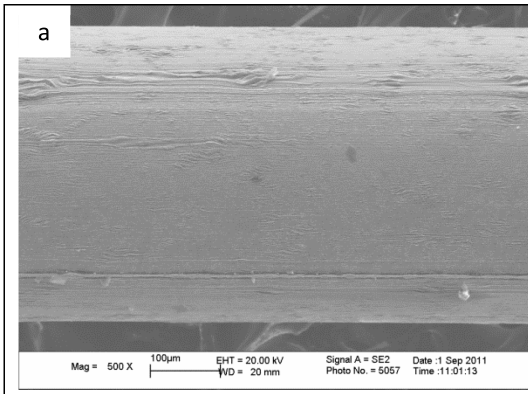

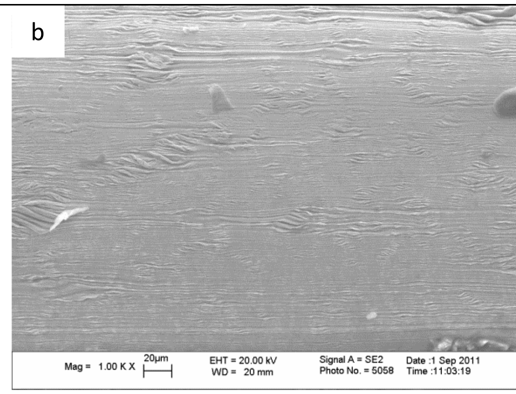

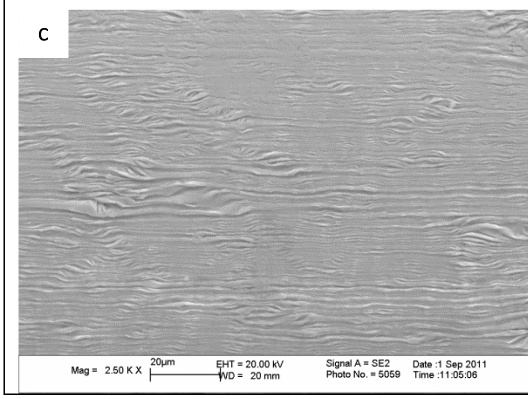

A Vitreloy 1 ($Zr_{41.2}Ti_{13.8}Cu_{12.5}Ni_{10}Be_{22.5}$) wire with thickness of approximately 420 μm.

a) 500x magnification
b) 1000x magnification
c) 2500x magnification

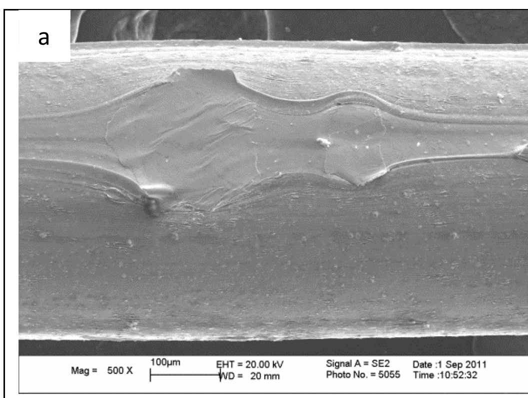

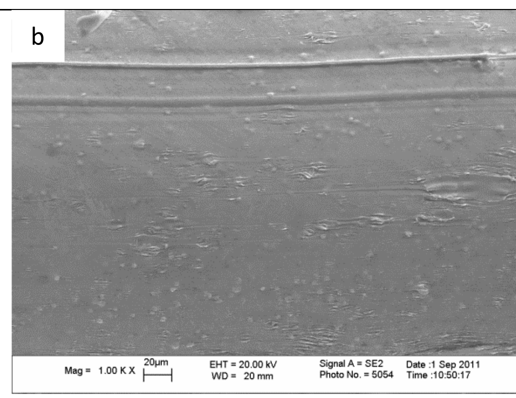

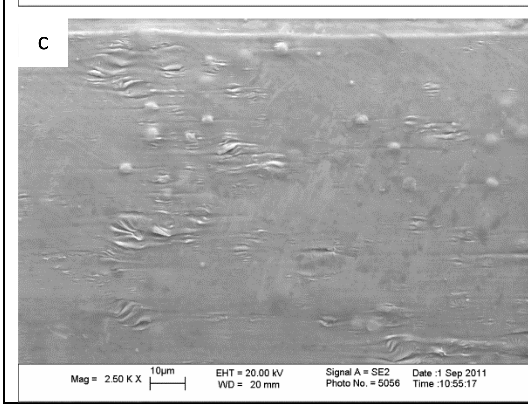

A Vitreloy 106 ($Zr_{57}Nb_{5}Al_{10}Cu_{15.4}Ni_{12.6}$) wire with thickness of approximately 425 mm.

a) 500x magnification
b) 1000x magnification
c) 2500x magnification

Coefficient of Thermal Expansion of BMGMC Composites

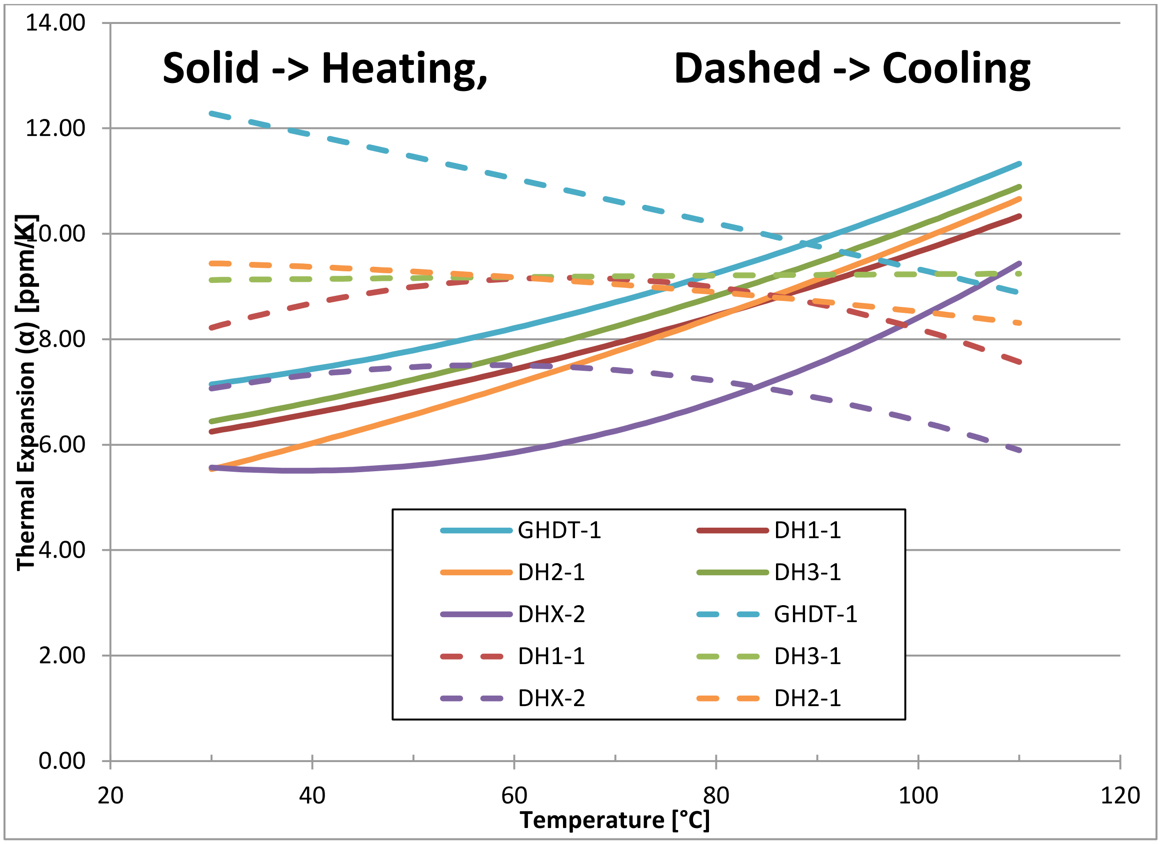

A series of BMGMC composites were alloyed, suction cast, sectioned, polished, and had their thermal expansion measured via TMA. Each alloy underwent a series of heating and cooling cycles. The average derivative of each alloy is shown above. Separate curves are given for heating and cooling.

Dendrite fractions should be as follows.

Alloy	Fraction Amorphous	Fraction Dendrite
GHDT	1	0
DH1	2/3	1/3
DH2	½	½
DH3	1/3	2/3
DHX	0	1

GHDT and DHX were taken as close approximations of the actual composition of the matrix and dendrites in the DH series of BMGMCs. At the time the precise composition could not be determined due to the beryllium content which could not be accurately measured.

Melt Spinner

In an attempt to further understand the corrosion properties of metallic glasses, a melt spinning apparatus was built to be able to vitrify a wide variety of MG systems. The idea behind a melt spinner is to eject a thin stream of molten alloy onto a rapidly spinning copper wheel. The wheel will rapidly quench the molten liquid at rates of up to 10^6 K/sec.

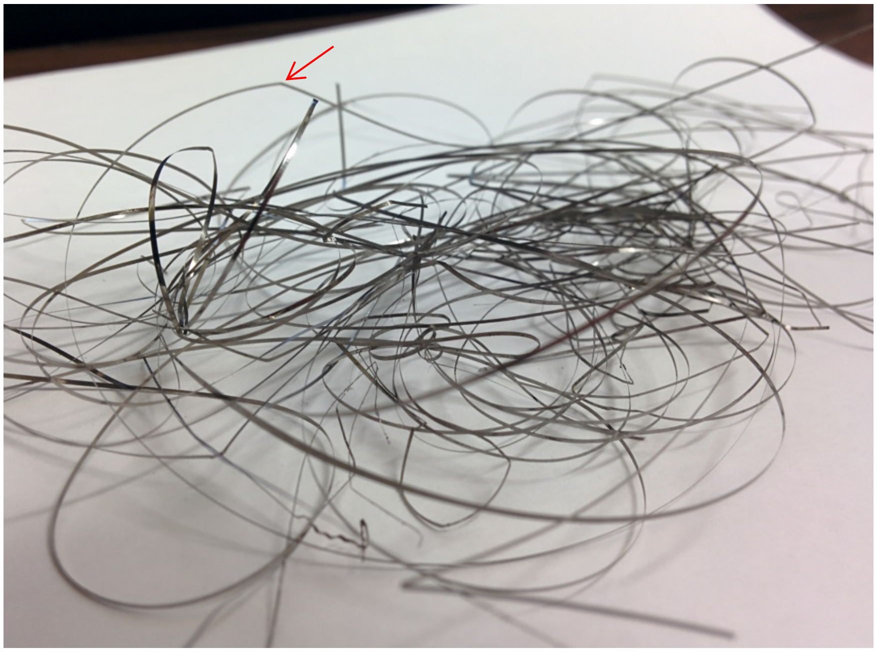

A successfully fabricated $Ni_{22}Zr_{78}$ wire. It is several meters long. The arrow points to a kink showing plasticity due to the wire's thickness being below twice the plastic zone size.

Unfortunately, the melt spinner met an untimely demise as the braising of the copper ring to the edge of the melt spinner failed in the middle of an experiment.

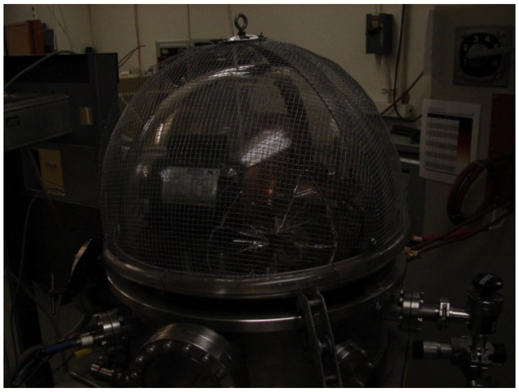
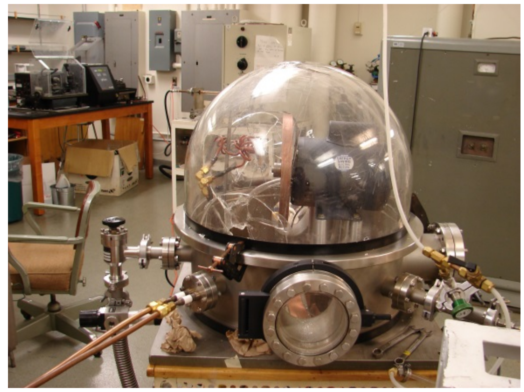
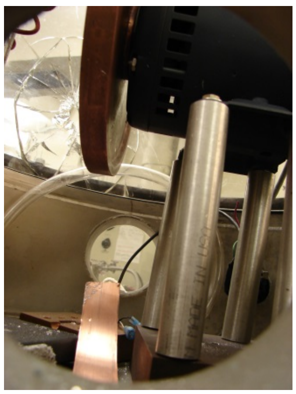
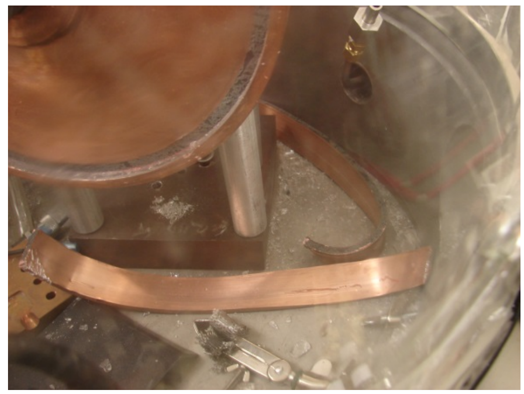

Unfortunately, the melt spinner met an untimely demise as the braising of the copper ring to the edge of the melt spinner failed in the middle of an experiment. In the end, the motor, bell jar, feedthroughs, ring stand, and clamp were all destroyed. The only surviving piece of the experiment was the feedstock ingot of metallic glass.